

1 **Title:** A transposon surveillance mechanism that safeguards plant male fertility during stress

2

3 **Authors:** Yang-Seok Lee¹, Robert Maple¹, Julius Dürr¹, Alexander Dawson¹, Saleh Tamim²,
4 Charo del Genio³, Ranjith Papareddy⁷, Anding Luo⁴, Jonathan C. Lamb⁵, Anne W. Sylvester⁴,
5 James A. Birchler⁵, Blake C. Meyers^{6,7}, Michael D. Nodine⁸, Jacques Rouster⁹ and Jose
6 Gutierrez-Marcos^{1*}

7

8 **Affiliations:**

9 ¹School of Life Sciences, University of Warwick, Coventry, CV4 7AL, UK,

10 ²Center for Bioinformatics and Computational Biology, University of Delaware, Newark, DE
11 19711, USA,

12 ³Centre for Fluid and Complex Systems, School of Computing, Electronics and Mathematics,
13 Coventry University, Prior Street, Coventry, CV1 5FB, UK,

14 ⁴Department of Molecular Biology University of Wyoming Department #3944 1000 E.
15 University Ave. Laramie, WY 82071, USA,

16 ⁵Division of Biological Sciences, University of Missouri, 311 Tucker Hall, Columbia, MO
17 65211, USA,

18 ⁶Donald Danforth Plant Science Center 975 N. Warson Rd., St. Louis, MO 63132, USA,

19 ⁷Division of Plant Sciences, University of Missouri, 52 Agriculture Lab, Columbia, MO
20 65211, USA,

21 ⁸Gregor Mendel Institute (GMI), Austrian Academy of Sciences, Vienna Biocenter (VBC),
22 Dr. Bohr-Gasse 3, 1030 Vienna, Austria,

23 ⁹Biogemma Centre de Recherche de Chappes Route d'Ennezat 63720 Chappes, France.

24 *To whom correspondence and request for material should be addressed.

25

26 **Abstract**

27 Although plants are able to withstand a range of environmental conditions, spikes in ambient
28 temperature can impact plant fertility causing reductions in seed yield and significant
29 economic losses^{1,2}. Therefore, understanding the precise molecular mechanisms that underpin
30 plant fertility under environmental constraints is critical to safeguard future food production³.
31 Here, we identified two Argonaute-like proteins whose activities are required to sustain male
32 fertility in maize plants under high temperatures. We found that MALE-ASSOCIATED
33 ARGONAUTE 1 and 2 (MAGO1 and MAGO2) associate with temperature-induced phased
34 secondary small RNAs in pre-meiotic anthers and are essential to control the activity of

35 retrotransposons in male meiocyte initials. Biochemical and structural analyses revealed how
36 MAGO2 activity and its interaction with retrotransposon RNA targets are modulated through
37 the dynamic phosphorylation of a set of highly conserved surface-located serine residues. Our
38 results demonstrate that an Argonaute-dependent RNA-guided surveillance mechanism is
39 critical in plants to sustain male fertility under environmentally constrained conditions by
40 controlling the mutagenic activity of transposons in male germ cells.

41

42 **Introduction:**

43 Crop yield loss driven by high temperatures has been widely reported in many species,
44 posing a real threat to food security^{2,4,5}. Plant male reproductive development is especially
45 sensitive to spikes in temperature⁶, with direct consequences on fertility and seed
46 productivity^{3,7}, likely due to metabolic and physiological changes resulting from epigenetic
47 perturbations triggered by heat stress⁸. In rice, the temperature-sensitive genic male sterile
48 mutants, *pms3* and *p/tms12-1*, have been found to carry mutations in long non-coding RNA
49 (lncRNA) precursors that normally produce phased secondary small interfering RNAs
50 (phasiRNAs)⁹⁻¹¹ mainly in developing anthers. The slicing of rice lncRNA phasiRNA (*PHAS*)
51 precursors is directed by two 22-nt miRNAs (miR2118 and miR2275)^{12,13}, leading to the
52 formation of double-stranded RNA by RNA-DEPENDENT RNA POLYMERASE 6
53 (RDR6)¹⁴, which is sequentially processed by Dicer-like (DCL) proteins DCL4 or DCL5 into
54 21- or 24-nt phasiRNAs, respectively^{15,16}. Interestingly, two rice Argonaute-like (AGO)
55 proteins, AGO 18 and MEIOSIS ARRESTED AT LEPTOTENE1 (MEL1) have been found
56 to be associated with 21-nt phasiRNAs and are required for male fertility^{13,17,18}. Thus, while
57 the production of phasiRNAs in rice anthers has been linked to male fertility, the precise
58 biological significance of this pathway in plants remains largely unknown.

59 It has been reported that maize anthers also accumulate two distinct populations of
60 phasiRNAs, which occur at distinct phases of male germ cell development¹⁹. Of particular
61 interest is the 21-nt phasiRNA subclass, which is abundant in the epidermis of pre-meiotic
62 wild type anthers but absent in male-sterile mutants lacking a functional anther epidermis^{19,20}.
63 We postulated that the pre-meiotic phasiRNA pathway might play a critical role in supporting
64 male fertility in plants. To this end, we scanned maize transcriptome data to identify
65 components of the sRNA pathway specifically expressed in the epidermis of pre-meiotic
66 anthers. We identified two Argonaute-like genes, with similarity to Arabidopsis AGO5 and
67 rice MEL1, which we named Male-Associated Argonaute 1 and 2 (MAGO1 and MAGO2)

68 (Fig S1A-B). Immunolocalization using specific antibodies revealed that MAGO1/2
69 accumulate primarily in the cytoplasm of epidermal cells of pre-meiotic anthers and in the
70 nuclei of developing meiocytes (Fig. S1C).

71 To determine the possible roles of MAGO1/2, we first identified transposon insertion mutant
72 alleles for both genes and found that while all wild-type and single mutant plants grown
73 under field conditions produced fully viable mature pollen, double mutant plants were male-
74 sterile (Fig. S2A-B). In addition, we generated *MAGO1/2* RNAi lines to simultaneously
75 downregulate both genes (*MAGO^{KD}*) (Fig. S2C) and found that most *MAGO^{KD}* lines
76 displayed a range of male sterility phenotypes under field-grown conditions (Fig. 1A and Fig.
77 S2D). Taken together, our genetic analyses revealed that both MAGO genes are required for
78 male fertility in maize.

79 Because the spatial and temporal accumulation of MAGO1/2 mirrors the reported expression
80 of 21-nt phasiRNAs and the predicted miR2118 trigger¹⁹, we next tested whether MAGO1/2
81 are involved in either the biogenesis or function of these phasiRNAs. We therefore performed
82 immunoprecipitations using specific antisera and sequencing the bound small RNAs. We
83 found that both MAGO1/2 are associated with the previously identified pre-meiotic 21-nt
84 phasiRNAs (Fig. S3A-C), however, the abundance of these sRNAs was not significantly
85 altered in *MAGO^{KD}* plants (Fig. S3D). This analysis revealed that MAGO1/2 are not directly
86 implicated in the biogenesis of these particular phasiRNAs.

87 Given that male germline pre-meiotic phasiRNAs in rice are implicated in heat stress
88 sensitivity and male fertility, we investigated the effects of heat stress on MAGO1/2 activity
89 in maize. To this end, we grew wild-type and *MAGO^{KD}* plants under control temperature
90 conditions and exposed them to a brief heat stress treatment either before or after male
91 meiosis. Pollen viability was not affected in *MAGO^{KD}* plants when grown under non-stress
92 (control) conditions, nor was it significantly affected in wild-type or *MAGO^{KD}* plants
93 exposed to heat stress after meiosis (Fig. S4A). However, heat stress applied before meiosis
94 had profound effects on pollen viability in *MAGO^{KD}* plants, becoming largely infertile, while
95 wild-type plants remained relatively unaffected (Fig. 1B and Fig. S4B). Taken together, our
96 genetic analyses revealed that both MAGO genes are required for male fertility under heat
97 stress. Further, we postulated that a new class of MAGO-associated pre-meiotic phasiRNAs
98 might determine male fertility under restrictive temperature conditions. To test this idea, we
99 sequenced sRNAs from pre-meiotic anthers after a short exposure to heat stress (72 h/35°C).
100 We found a massive accumulation of a discrete group of 21-nt phasiRNAs (Hphasi) in wild-

101 type plants, but not in MAGO^{KD} plants (Fig. 1C and Fig. S5). Analysis of uncapped RNA
102 ends provided strong evidence for miR2118-directed cleavage of Hphasi lncRNA precursors
103 in pre-meiotic wild-type anthers (Fig. S6). The spatial distribution of these sRNAs was
104 determined by RNA *in situ* localisation on anther sections from wild-type plants grown under
105 permissive and restrictive conditions (Fig. 1D). We found that heat stress triggered Hphasi
106 accumulation, primarily in the epidermis of pre-meiotic anthers and also in the inner anther
107 cell layers at the onset of meiosis. However, we did not observe any increase in the
108 accumulation of miR2118 in pre-meiotic anthers after heat stress. We therefore sought to
109 determine whether the biogenesis of these RNAs play a role in male fertility. Given that HC-
110 Pro can directly bind and sequester small RNAs^{21,22}, we reasoned that HC-Pro induction in
111 heat-stressed pre-meiotic anthers could interfere with the biogenesis and/or function of this
112 particular class of phasiRNAs. Therefore to test this hypothesis, we first generated transgenic
113 plants carrying a dexamethasone (DEX)-inducible viral gene-silencing suppressor – Helper
114 Component-Proteinase (HC-Pro)^{23,24}. We next immunoprecipitated HC-Pro from DEX-
115 treated anthers and sequenced the bound sRNAs. We found that HC-Pro expression in pre-
116 meiotic anthers was associated with 21-nt phasiRNAs and their predicted miR2188 trigger
117 (Fig. S7A-D). To further define the role(s) of these sRNAs, HC-Pro was ectopically
118 expressed in anthers before and after meiosis. Pre-meiotic induction resulted in a near
119 complete lack of pollen grains at anther maturity, whereas post-meiotic HC-Pro induction
120 exerted only minor effects on pollen production (Fig. S7E). To establish whether the HC-Pro-
121 mediated effects on male fertility were specifically linked to sRNAs produced in anther
122 epidermal tissues, we generated maize plants with HC-Pro under the control of an epidermal-
123 specific HDZIV6 trans-activation system (HDZIV6>>HC-Pro) and confirmed exclusive HC-
124 Pro expression in the anther epidermis by immunolocalization using a specific HC-Pro
125 antibody that we generated (Fig. 1E-F). Notably, we found that the production of pollen
126 grains in HDZIV6>>HC-Pro plants was drastically reduced compared to control plants (Fig.
127 1G). Collectively, these data provide evidence for the activation of a specific sRNA cascade
128 in anther epidermis that is critical to support male fertility under restrictive temperature-stress
129 conditions.

130 Computational genome-wide scans showed that Hphasi mapped primarily to transposable
131 elements (TEs) and specifically to long terminal repeat retrotransposons (LTRs) within the
132 maize genome (Fig. S8A-B). Because TEs are typically deregulated in plants during periods
133 of genome shock or abiotic stress²⁵, we reasoned that the HphasiRNAs might be involved in

134 the silencing of TEs in anthers following environmental stress exposure. To test this
135 hypothesis, we performed RNA sequencing (RNA-seq) to compare global changes in gene
136 expression in pre-meiotic anthers of $MAGO^{KD}$ and wild-type plants. Under permissive
137 conditions, we did not observe any significant changes in the anther-specific expression of
138 coding genes between WT and $MAGO^{KD}$ (Fig. S8C). By contrast, exposure to heat stress
139 before meiosis resulted in global changes in anther gene expression in all plants tested
140 independent of genotype (Fig. S8C-D and Table S1). Notably, we found that LTR
141 retrotransposons were significantly deregulated in anthers and in meiocytes of $MAGO^{KD}$
142 plants after heat stress (Fig. 2A-B). In addition, most of the retrotransposons upregulated in
143 heat-stressed $MAGO^{KD}$ plants were of the low-copy Gypsy (LRGs) class predicted to be
144 targeted by Hphasi (Fig. S9A and Table S2). Subsequent analysis of uncapped RNA ends
145 provided strong support for the directed cleavage of LRGs by Hphasi (Fig. 2C and Fig. S9B).
146 To test if MAGO and associated phasiRNAs are involved in modulating the mobility of these
147 LRGs, we carried out transposon display and retrotransposon-sequence capture on progenies
148 generated from reciprocal crosses between wild-type and $MAGO^{KD}$ plants grown under
149 permissive conditions. These analyses revealed retrotransposons to be highly mobile only in
150 the male germ cell lineage of $MAGO^{KD}$ plants (Fig. 2D and Table S3).

151 Our data thus far point to a role for MAGO proteins in protecting male germ cells from the
152 deregulated activity of retrotransposons that occurs during heat stress. In order to understand
153 how MAGO activity is regulated by heat stress, we first analysed our RNAseq data. However,
154 we did not observe significant changes in transcript levels in response to heat stress,
155 indicating that MAGO activity may be modulated post-translationally. Indeed, previous
156 studies in maize and rice have identified other Argonaute-like proteins that are
157 phosphorylated in anthers^{26,27}. We therefore performed a phosphoproteome analysis of pre-
158 meiotic wild-type anthers and identified major changes in phosphorylation induced by short
159 exposure to heat stress (Fig. 3A and Table S4). Specifically, a region in the PIWI domain of
160 MAGO2 that contains four serines (S989, S990, S994 and S998) and one threonine (T995)
161 residue was significantly hypo-phosphorylated in response to heat stress (Figure S10). To
162 further understand the biological significance of these dynamic changes in MAGO2
163 phosphorylation, we modelled the structure of the conserved catalytic domain of MAGO2
164 and analysed the electrostatic potential of the molecular surface of different phosphorylation
165 variants (Fig. 3B and Movie). We found that the residues targeted by phosphorylation are
166 located at the surface of a loop following the PIWI domain (Fig. S11A). This finding is in

167 line with the conserved presence of phosphorylated serine/threonine residues in the PIWI
168 loops of other catalytically active plant and animal Argonautes (Fig. S11B and Table S5).
169 These phosphorylated residues are in close proximity to the central cleft and to an L2 loop,
170 which are considered important for the regulation of sRNA:target interactions²⁸. Notably, we
171 found that the hyper-phosphorylation of S989-S998 does not cause significant changes to
172 MAGO2 structure, however is predicted to cause profound changes to the electrostatic
173 surface potential of the upper central cleft region (Fig. 3B). To test if these stress-induced
174 changes could affect the affinity for sRNAs and/or the enzymatic activity of MAGO2, we
175 immunoprecipitated MAGO2 from anthers of plants exposed to a pulse of heat stress prior to
176 meiosis and quantified the bound small RNAs. While we did not find significant differences
177 in the association of MAGO2 with 21-nt Hphasi under control and heat-stress conditions (Fig.
178 3C), the abundance of retrotransposon RNA targets associated with MAGO2 was
179 significantly reduced after exposure to heat stress (Fig. 3D). Because of this, we reasoned that
180 the changes in surface charge brought about by MAGO2 hypo-phosphorylation could
181 regulate the interaction between sRNA and target to sustain the rapid silencing of deregulated
182 retrotransposons in the male germ cells. To test this hypothesis, we generated an *in vivo*
183 reporter system to test the catalytic activity of wild-type MAGO2 and a series of
184 phosphoresistant (S>A) and phosphomimetic (S>E) MAGO2 mutants (Fig. S12). We also
185 generated mutations in MAGO2 residues predicted to be essential for sRNA binding (Y676E)
186 and small RNA-directed RNA cleavage (D835E) for inclusion in this experiment. We found
187 that while sRNA binding was affected in MAGO^{Y676E}, it was not significantly affected in
188 either MAGO^{S>A}, MAGO^{S>E} or MAGO^{D835E} (Fig. 3E). Silencing activity was, however,
189 abolished in MAGO^{Y676E} and significantly reduced in only MAGO^{S>E} (Fig. 3F). These data
190 suggest that stress-mediated hypo-phosphorylation of MAGO2 is important for its effective
191 interaction with retrotransposon RNA targets. This model is consistent with previous studies
192 in humans, which have shown that hyper-phosphorylation of the PIWI domain of AGO2
193 (S824–S834) impairs RNA:target association while hypo-phosphorylation expands the target
194 repertoire^{29,30}.

195 In sum, we have identified in maize two Argonaute-like proteins acting alongside a distinct
196 group of sRNAs in a male germline-specific manner. This pathway is remarkably similar to
197 the small RNA-mediated recognition pathway found in mammalian male germ cells, which
198 acts to silence retrotransposon activity³¹. Unlike in animals, transposon activity is however
199 more permissive in plants. For instance, bursts of transposon mobility have helped shape

200 plant genomes and alter transcriptional responses³². Further, the insertion of retrotransposons
201 in gene regulatory regions have caused notable dramatic effects on plant phenotypes – a
202 property that was repeatedly exploited during the process of crop domestication³³.
203 Nevertheless, plants must regulate retrotransposon activity because, as shown for genomic
204 shock, deregulated retrotransposon activity often results in genomic and epigenomic
205 instability, and ultimately causes negative effects on offspring fitness²⁵. Our findings reveal
206 an Argonaute-mediated pathway that protects plant male fertility by acting as a pre-meiotic
207 surveillance mechanism activated in the somatic cells that surround the germ cell precursors.
208 The biological significance of this molecular pathway operating under heat stress conditions
209 to restrict retrotransposon activity in developing male germ cells may be to prevent the
210 widespread transmission of unwanted or deleterious mutations in wind-pollinated plants such
211 as grasses³⁴⁻³⁶. The manipulation of this molecular mechanism in crops will undoubtedly
212 become a useful strategy in future efforts to enhance male fertility and sustain seed
213 productivity under unpredictable and stressful climate conditions.

214

215 **Acknowledgements:**

216 We thank Gary Grant and Peter Watson for help with plant husbandry; Liliana M. Costa for
217 discussions and comments on the manuscript. This research was supported by awards from
218 US National Science Foundation (1027445 to A.W.S. and 1649424 & 1754097 to B.M.),
219 European Research Council (Grant 637888 to M.D.N.) and BBSRC (BB/L003023/1,
220 BB/N005279/1, BB/N00194X/1 and BB/P02601X/1) to J.G-M.

221

222 **Author Contributions:**

223 Y-S. L. and R.M. cultivated plants, harvested samples and collected phenotypic data. R.P.,
224 JG-M and J.R. identified transposon insertions. J.D. performed the phosphoproteome analysis.
225 R.M. and Y-S. L. performed immunoprecipitation and small-RNA-seq libraries. A.L. and J.L.
226 generated constructs and transgenic lines for HC-Pro and HDZIV6 transactivation. R.P.
227 constructed nanoPARE libraries. R.M, A.D, S.T. and M.D.N. performed the bioinformatic
228 analysis. C. de G. performed the molecular dynamics simulation and protein modelling. Y-S.
229 L., R.M., Y.D, A.D., S.T., C. de G. prepared figures and tables. A.W.S, J.B., B.C.M., M.D.N.,
230 J.R. and J.G-M. co-ordinated experiments. Y-S. L. and R.M. and J.G-M. conceived the
231 project. J.G-M. wrote the manuscript with input from the rest of the authors.

232

233 **Competing interest:** The authors declare that they have no competing interests.

234

235 **Data and Materials Availability:** Sequence data (mRNA-seq, nanoPARE-seq, sRNAseq
236 and LTR-seq) that support the findings of this study have been deposited at the European
237 Nucleotide Archive (ENA) under the accession code ERP118841.

238

239 **List of Supplemental Materials:**

240 Materials and Methods

241 Figures S1-S11

242 Tables S1-S7

243 Movie 1

244

245 **References and Notes:**

246 1 Challinor, A. J. *et al.* A meta-analysis of crop yield under climate change and
247 adaptation. *Nature Climate Change* **4**, 287, doi:10.1038/nclimate2153

248 <https://www.nature.com/articles/nclimate2153#supplementary-information> (2014).

249 2 Peng, S. *et al.* Rice yields decline with higher night temperature from global warming.
250 *Proc Natl Acad Sci U S A* **101**, 9971-9975, doi:10.1073/pnas.0403720101 (2004).

251 3 Hedhly, A., Hormaza, J. I. & Herrero, M. Global warming and sexual plant
252 reproduction. *Trends Plant Sci* **14**, 30-36, doi:10.1016/j.tplants.2008.11.001 (2009).

253 4 Challinor, A. J. *et al.* A meta-analysis of crop yield under climate
254 change and adaptation. *Nature Climate Change* **4** (2014).

255 5 Lobell, D. B. & Asner, G. P. Climate and management contributions to recent trends
256 in U.S. agricultural yields. *Science* **299**, 1032, doi:10.1126/science.1077838 (2003).

257 6 De Storme, N. & Geelen, D. The impact of environmental stress on male
258 reproductive development in plants: biological processes and molecular mechanisms.
259 *Plant Cell Environ* **37**, 1-18, doi:10.1111/pce.12142 (2014).

260 7 Barnabas, B., Jager, K. & Feher, A. The effect of drought and heat stress on
261 reproductive processes in cereals. *Plant Cell Environ* **31**, 11-38, doi:10.1111/j.1365-
262 3040.2007.01727.x (2008).

263 8 Begcy, K. & Dresselhaus, T. Epigenetic responses to abiotic stresses during
264 reproductive development in cereals. *Plant Reprod* **31**, 343-355,
265 doi:10.1007/s00497-018-0343-4 (2018).

266 9 Ding, J. *et al.* A long noncoding RNA regulates photoperiod-sensitive male sterility,
267 an essential component of hybrid rice. *Proc Natl Acad Sci U S A* **109**, 2654-2659,
268 doi:10.1073/pnas.1121374109 (2012).

269 10 Fan, Y. *et al.* PMS1T, producing phased small-interfering RNAs, regulates
270 photoperiod-sensitive male sterility in rice. *Proc Natl Acad Sci U S A* **113**, 15144-
271 15149, doi:10.1073/pnas.1619159114 (2016).

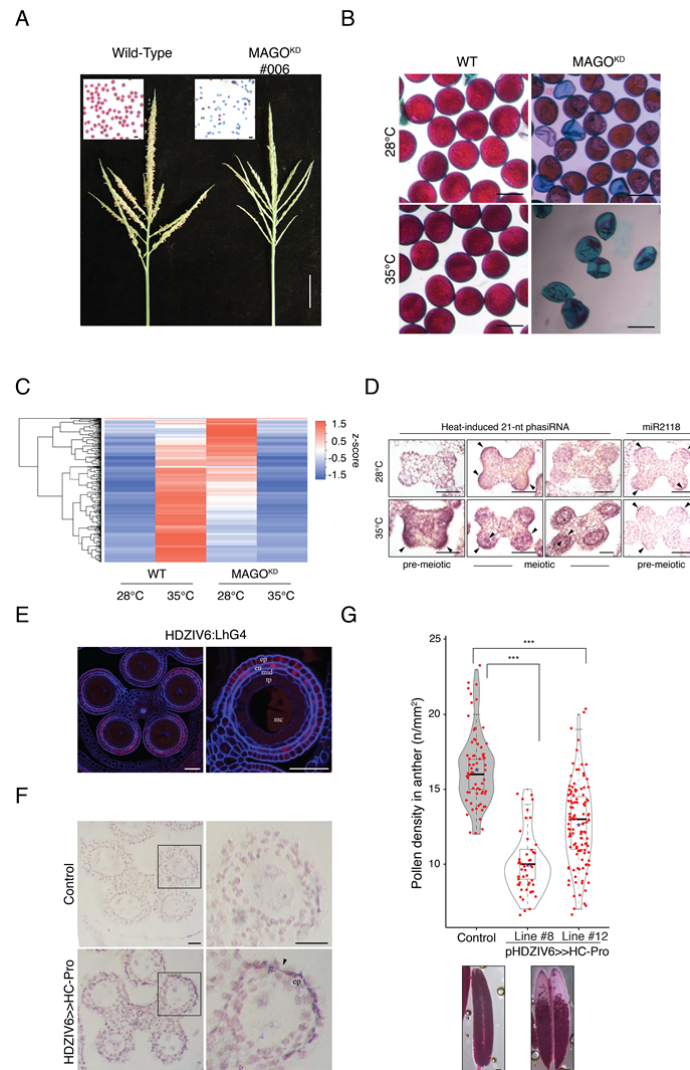
272 11 Zhou, H. *et al.* Photoperiod- and thermo-sensitive genic male sterility in rice are
273 caused by a point mutation in a novel noncoding RNA that produces a small RNA.
274 *Cell Res* **22**, 649-660, doi:10.1038/cr.2012.28 (2012).

275 12 Johnson, C. *et al.* Clusters and superclusters of phased small RNAs in the developing
276 inflorescence of rice. *Genome Res* **19**, 1429-1440, doi:10.1101/gr.089854.108 (2009).

- 277 13 Komiya, R. *et al.* Rice germline-specific Argonaute MEL1 protein binds to phasiRNAs
278 generated from more than 700 lincRNAs. *Plant J* **78**, 385-397, doi:10.1111/tpj.12483
279 (2014).
- 280 14 Song, X. *et al.* Rice RNA-dependent RNA polymerase 6 acts in small RNA biogenesis
281 and spikelet development. *Plant J* **71**, 378-389, doi:10.1111/j.1365-
282 313X.2012.05001.x (2012).
- 283 15 Song, X. *et al.* Roles of DCL4 and DCL3b in rice phased small RNA biogenesis. *Plant J*
284 **69**, 462-474, doi:10.1111/j.1365-313X.2011.04805.x (2012).
- 285 16 Xia, R. *et al.* 24-nt reproductive phasiRNAs are broadly present in angiosperms. *Nat*
286 *Commun* **10**, 627, doi:10.1038/s41467-019-08543-0 (2019).
- 287 17 Das, S., Swetha, C., Pachamuthu, K., Nair, A. & Shivaprasad, P. V. Loss of function of
288 *Oryza sativa* Argonaute 18 induces male sterility and reduction in phased small RNAs.
289 *Plant Reprod* **33**, 59-73, doi:10.1007/s00497-020-00386-w (2020).
- 290 18 Nonomura, K. *et al.* A germ cell specific gene of the ARGONAUTE family is essential
291 for the progression of premeiotic mitosis and meiosis during sporogenesis in rice.
292 *Plant Cell* **19**, 2583-2594, doi:10.1105/tpc.107.053199 (2007).
- 293 19 Zhai, J. *et al.* Spatiotemporally dynamic, cell-type-dependent premeiotic and meiotic
294 phasiRNAs in maize anthers. *Proc Natl Acad Sci U S A* **112**, 3146-3151,
295 doi:10.1073/pnas.1418918112 (2015).
- 296 20 Vernoud, V. *et al.* The HD-ZIP IV transcription factor OCL4 is necessary for trichome
297 patterning and anther development in maize. *Plant J* **59**, 883-894,
298 doi:10.1111/j.1365-313X.2009.03916.x (2009).
- 299 21 Shibolet, Y. M. *et al.* The conserved FRNK box in HC-Pro, a plant viral suppressor of
300 gene silencing, is required for small RNA binding and mediates symptom
301 development. *J Virol* **81**, 13135-13148, doi:10.1128/JVI.01031-07 (2007).
- 302 22 Lakatos, L. *et al.* Small RNA binding is a common strategy to suppress RNA silencing
303 by several viral suppressors. *EMBO J* **25**, 2768-2780, doi:10.1038/sj.emboj.7601164
304 (2006).
- 305 23 Kasschau, K. D. & Carrington, J. C. A counterdefensive strategy of plant viruses:
306 suppression of posttranscriptional gene silencing. *Cell* **95**, 461-470,
307 doi:10.1016/s0092-8674(00)81614-1 (1998).
- 308 24 Anandalakshmi, R. *et al.* A viral suppressor of gene silencing in plants. *Proc Natl Acad*
309 *Sci U S A* **95**, 13079-13084, doi:10.1073/pnas.95.22.13079 (1998).
- 310 25 Lisch, D. How important are transposons for plant evolution? *Nat Rev Genet* **14**, 49-
311 61, doi:10.1038/nrg3374 (2013).
- 312 26 Ye, J. *et al.* Proteomic and phosphoproteomic analyses reveal extensive
313 phosphorylation of regulatory proteins in developing rice anthers. *Plant J* **84**, 527-
314 544, doi:10.1111/tpj.13019 (2015).
- 315 27 Walley, J. W. *et al.* Integration of omic networks in a developmental atlas of maize.
316 *Science* **353**, 814-818, doi:10.1126/science.aag1125 (2016).
- 317 28 Sheu-Gruttaduria, J., Xiao, Y., Gebert, L. F. & MacRae, I. J. Beyond the seed:
318 structural basis for supplementary microRNA targeting by human Argonaute2. *EMBO*
319 *J* **38**, e101153, doi:10.15252/embj.2018101153 (2019).
- 320 29 Quevillon Huberdeau, M. *et al.* Phosphorylation of Argonaute proteins affects mRNA
321 binding and is essential for microRNA-guided gene silencing in vivo. *EMBO J* **36**,
322 2088-2106, doi:10.15252/embj.201696386 (2017).

- 323 30 Golden, R. J. *et al.* An Argonaute phosphorylation cycle promotes microRNA-
324 mediated silencing. *Nature* **542**, 197-202, doi:10.1038/nature21025 (2017).
- 325 31 Ernst, C., Odom, D. T. & Kutter, C. The emergence of piRNAs against transposon
326 invasion to preserve mammalian genome integrity. *Nat Commun* **8**, 1411,
327 doi:10.1038/s41467-017-01049-7 (2017).
- 328 32 Naito, K. *et al.* Unexpected consequences of a sudden and massive transposon
329 amplification on rice gene expression. *Nature* **461**, 1130-1134,
330 doi:10.1038/nature08479 (2009).
- 331 33 Studer, A., Zhao, Q., Ross-Ibarra, J. & Doebley, J. Identification of a functional
332 transposon insertion in the maize domestication gene *tb1*. *Nat Genet* **43**, 1160-1163,
333 doi:10.1038/ng.942 (2011).
- 334 34 Carpentier, M. C. *et al.* Retrotranspositional landscape of Asian rice revealed by 3000
335 genomes. *Nat Commun* **10**, 24, doi:10.1038/s41467-018-07974-5 (2019).
- 336 35 Dooner, H. K. *et al.* Spontaneous mutations in maize pollen are frequent in some
337 lines and arise mainly from retrotranspositions and deletions. *Proc Natl Acad Sci U S*
338 *A* **116**, 10734-10743, doi:10.1073/pnas.1903809116 (2019).
- 339 36 Peng, Y. *et al.* Elimination of a Retrotransposon for Quenching Genome Instability in
340 Modern Rice. *Mol Plant* **12**, 1395-1407, doi:10.1016/j.molp.2019.06.004 (2019).
- 341
- 342

343



344

345 **Fig. 1. MAGO and pre-meiotic small RNAs are essential for male fertility in maize.**

346 (A) Male fertility defects observed in MAGO^{KD} plants grown under field conditions. Pollen grains
347 after Alexander's Staining and mature male inflorescences. Scale bars are 200 μ m and 5 cm.

348 (B) Pollen viability in wild-type and MAGO^{KD} plants under permissive conditions (28°C) and
349 subjected to heat stress (35°C) before meiosis (n= 10). Scale bars are 200 μ m.

350 (C) Accumulation of 21-nt phasiRNAs in anthers of wild-type and MAGO^{KD} plants exposed to heat
351 stress before meiosis. n \geq 2 biologically independent samples each.

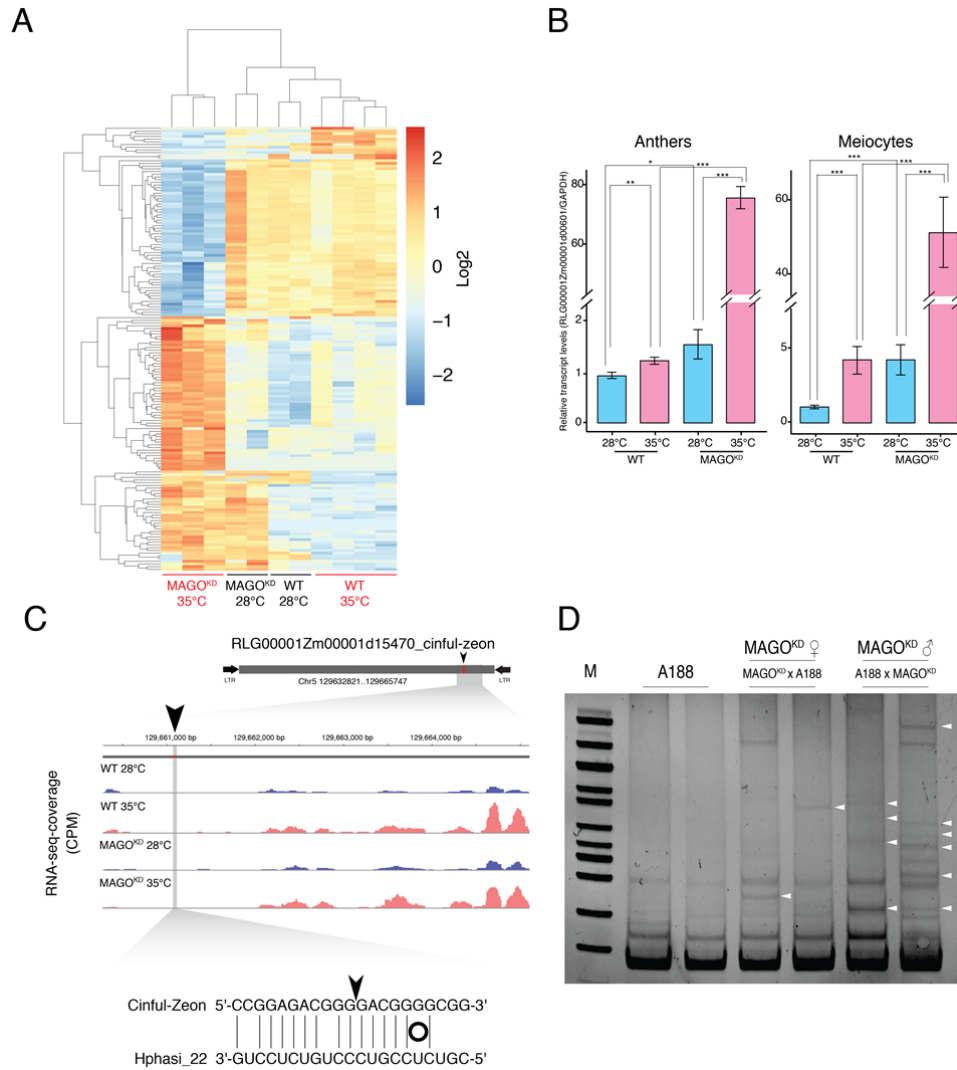
352 (D) *in situ* RNA localization of 21-nt Hphasi and miR2118 in anthers of wild-type plants exposed to
353 heat stress before meiosis. Scale bars are 50 μ m. Black arrowhead indicates accumulation of sRNAs

354 (E) Confocal images of NLS-dTomato reporter expression in anthers of HDZIV6>>HC-Pro plants.
355 Scale bars are 50 μ m. ep, epidermis; en, endothecium; mid, mid-layer; tp, tapetum; mc, meiocyte.

356 (F) Immunodetection of HC-Pro in anther epidermis in control and HDZIV6>>HC-Pro plants. Scale
357 bars are 50 μ m. Black arrowhead, accumulation of HC-Pro.

358 (G) Pollen viability in anthers from two independent HDZIV6>>HC-Pro lines (n \geq 30). Differences
359 between groups were determined by one-way ANOVA, ***p < 0.001. Black lane, median; Red star,
360 mean. Below, representative anthers after Alexander's Staining. Scale bars 100 μ m.

361



362
363
364
365
366
367
368
369
370
371
372
373
374
375
376
377
378
379
380
381

Fig. 2. MAGO1/2 are necessary to silence stress-activated retrotransposons in maize male germ cells.

(A) Heatmap analysis of transposon transcripts deregulated in anthers of wild-type and $MAGO^{KD}$ plants exposed to heat stress before meiosis. $n \geq 2$ biologically independent samples each.

(B) Relative expression of a MAGO regulated LTR in anthers and meiocytes of wild-type and $MAGO^{KD}$ plants exposed to heat stress before meiosis ($n = 4$). Differences between groups were determined by one-way ANOVA, * $p < 0.05$; ** $p < 0.01$; *** $p < 0.001$. Black lane, median; Red star, mean.

(C) Coverage of RNA-seq of retrotransposons targeted by Hphasi in anthers of wild-type and $MAGO^{KD}$ plants exposed to heat stress before meiosis. $n \geq 2$ biologically independent samples each. Black arrowhead and red box indicate the location of predicted sites for Hphasi-directed slicing remnants. $n = 3$ independent samples each. Grey box, retrotransposon; Black arrow, long terminal inverted repeats.

(D) Transposon display showing the presence of retrotransposon insertions in progenies from wild-type (A188) plants and from reciprocal crosses with $MAGO^{KD}$. Each lane represents a pool of 25 independent plants. $n = 2$ biologically independent experiments. White arrowheads indicate new retrotransposon insertions.

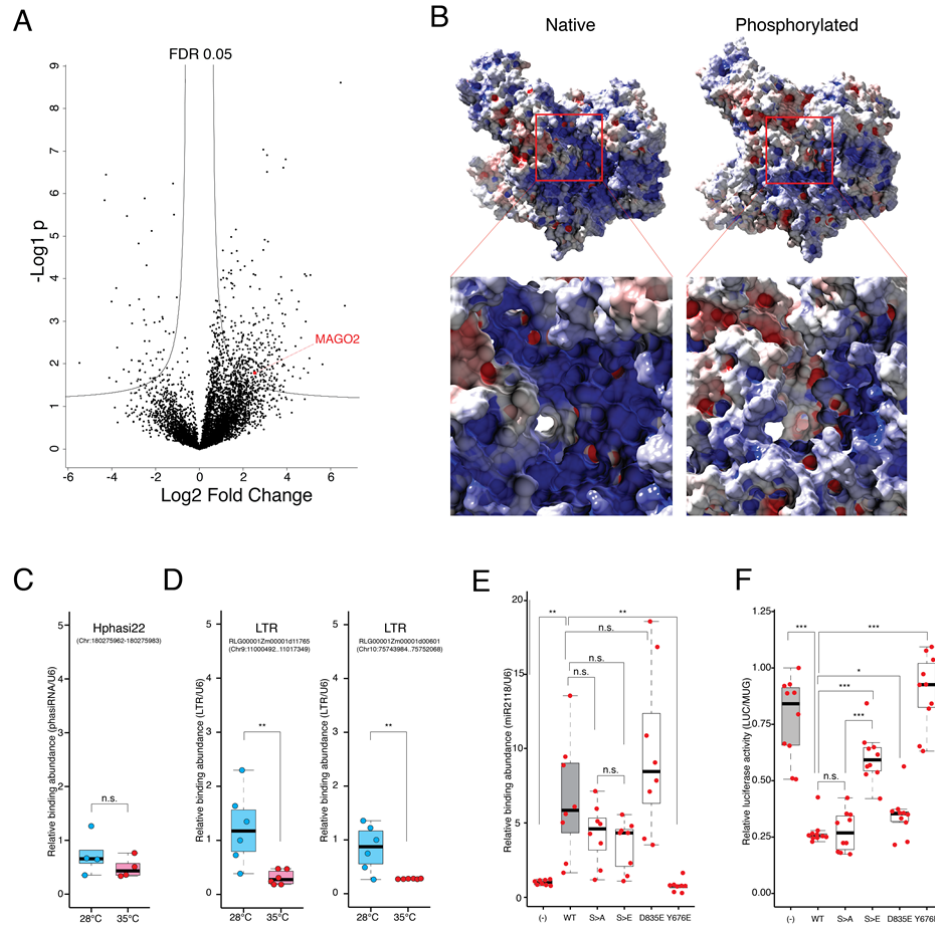


Fig. 3. MAGO activity is modulated by dynamic changes in phosphorylation induced by heat stress.

(A) Volcano plot showing dynamic changes in phosphorylation in premeiotic anthers after heat stress and identification of MAGO2 as a differentially phosphorylated protein. Threshold $FDR < 0.05$; Log_2 fold change > 1.5 ; $n = 6$ independent biological replicates. Red circle, MAGO2 phosphopeptides.

(B) Electrostatic potential distribution on the molecular surface of native and phosphorylated MAGO2 showing negative (red), positive (blue) and hydrophobic (grey) residues. Red boxes- close views of the central cleft and L2 loop known to be implicated in the regulation of sRNA:target interactions.

(C) Accumulation of Hphasi22 bound to MAGO2, shown by immunoprecipitation coupled to reverse-transcriptase polymerase chain reaction (qRT-PCR), in pre-meiotic anthers from wild-type plants exposed to control (28°C) and heat-stress conditions (35°C). $n = 4$ independent biological replicates. Differences between groups were determined by paired t-test, n.s. not significant.

(D) Accumulation of retrotransposon RNA bound to MAGO2, shown by immunoprecipitation coupled to reverse-transcriptase polymerase chain reaction (qRT-PCR), in pre-meiotic anthers from wild-type plants exposed to control (28°C) and heat-stress conditions (35°C). $n = 6$ independent biological replicates. Differences between groups were determined by paired t-test, $**p < 0.01$.

(E) Silencing activity of MAGO2 in wild-type and MAGO2 mutants for residues implicated in differential phosphorylation (S>A and S>E), and in residues predicted to be necessary for target cleavage (D835E) and sRNA binding (Y676E). $n = 10$ independent biological replicates. Differences between groups were determined by one-way ANOVA, $*p < 0.05$; $***p < 0.001$; n.s. not significant.

(F) Abundance of bound sRNAs in wild-type MAGO2 and mutants, shown by immunoprecipitation coupled to reverse-transcriptase polymerase chain reaction (qRT-PCR). $n = 10$ independent biological replicates. Differences between groups were determined by one-way ANOVA, $**p < 0.01$; n.s. not significant.

382
383

384
385

386
387

388
389

390
391

392
393

394
395

396
397

398
399

400
401

402
403

404
405

406
407